

Supporting Information

Pure and Intense Orange Upconversion Luminescence of Eu^{3+} from the Sensitization of Yb^{3+} - Mn^{2+} Dimer in $\text{NaY}(\text{Lu})\text{F}_4$ Nanocrystals

Zhuo Wang,^{ab} Jing Feng,^{*a} Shuyan Song,^a Zhiqiang Sun,^c Shuang Yao,^a Xin Ge,^a
Min Pang^{ab} and Hongjie Zhang^{*a}

^a State Key Laboratory of Rare Earth Resource Utilization, Changchun Institute of Applied Chemistry, Chinese Academy of Sciences, 5625 Renmin Street, Changchun 130022, China

^b University of Chinese Academy of Sciences, Beijing 100049, China

^c Cancer Hospital of Jilin Province, Changchun 130021, China

* Corresponding Authors

Email: fengj@ciac.ac.cn (Jing Feng), hongjie@ciac.ac.cn (Hongjie Zhang)

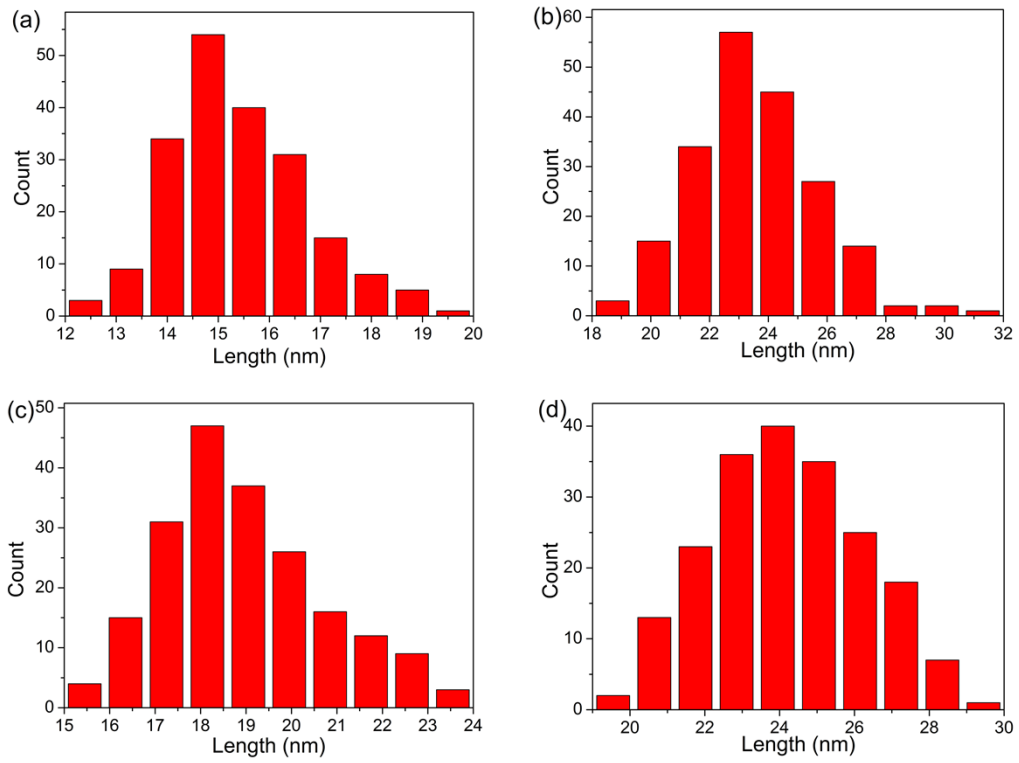


Fig. S1 Size histograms of (a) NaYF₄:Yb³⁺/Mn²⁺/Eu³⁺ (5/30/15 mol%) core and (b) core-shell NCs and (c) NaLuF₄:Yb³⁺/Mn²⁺/Eu³⁺ (5/30/15 mol%) core and (d) core-shell NCs.

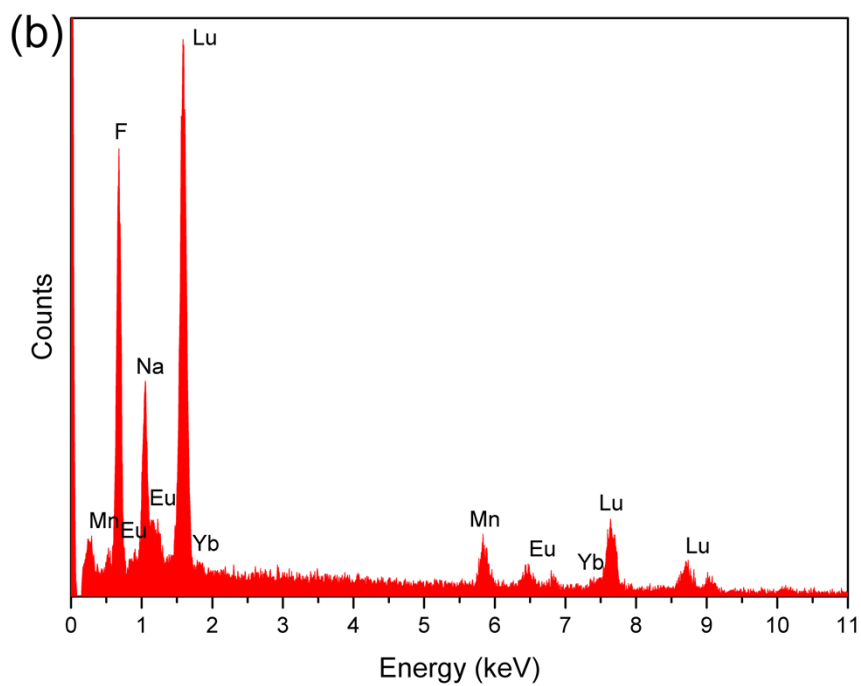
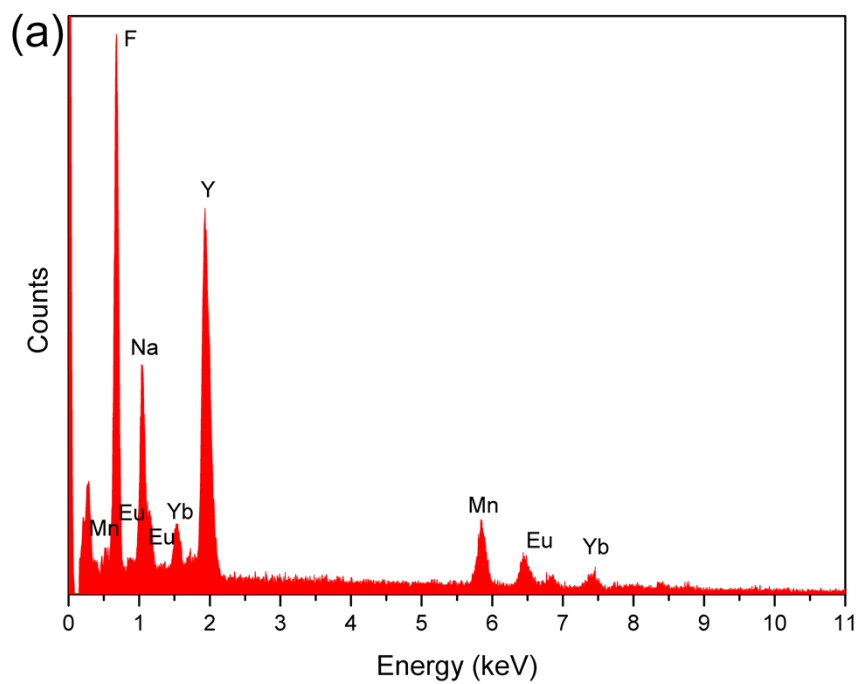


Fig. S2 EDX spectroscopy of (a) NaYF₄:Yb³⁺/Mn²⁺/Eu³⁺ (5/30/15 mol%) NCs and (b) NaLuF₄:Yb³⁺/Mn²⁺/Eu³⁺ (5/30/15 mol%) NCs.

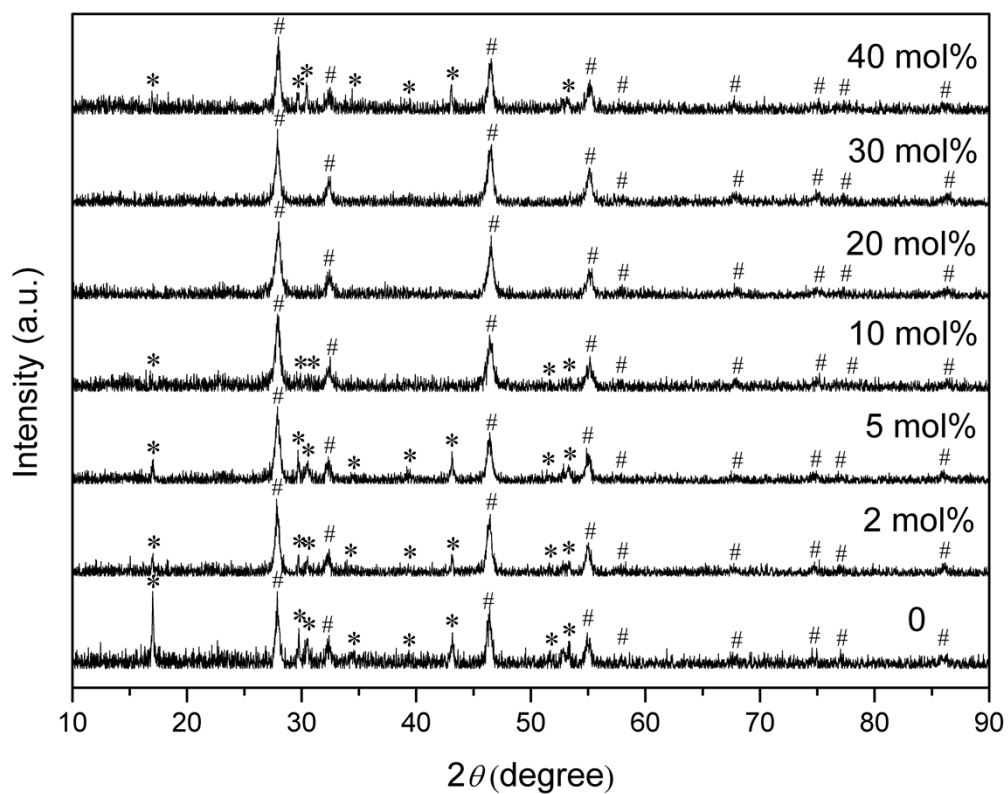


Fig. S3 XRD patterns of NaYF₄:Yb³⁺/Mn²⁺/Eu³⁺ (5/y/15 mol%) (y = 0-40) NCs.

Symbols # and * represent the standard diffraction peaks of α-NaYF₄ and β-NaYF₄.

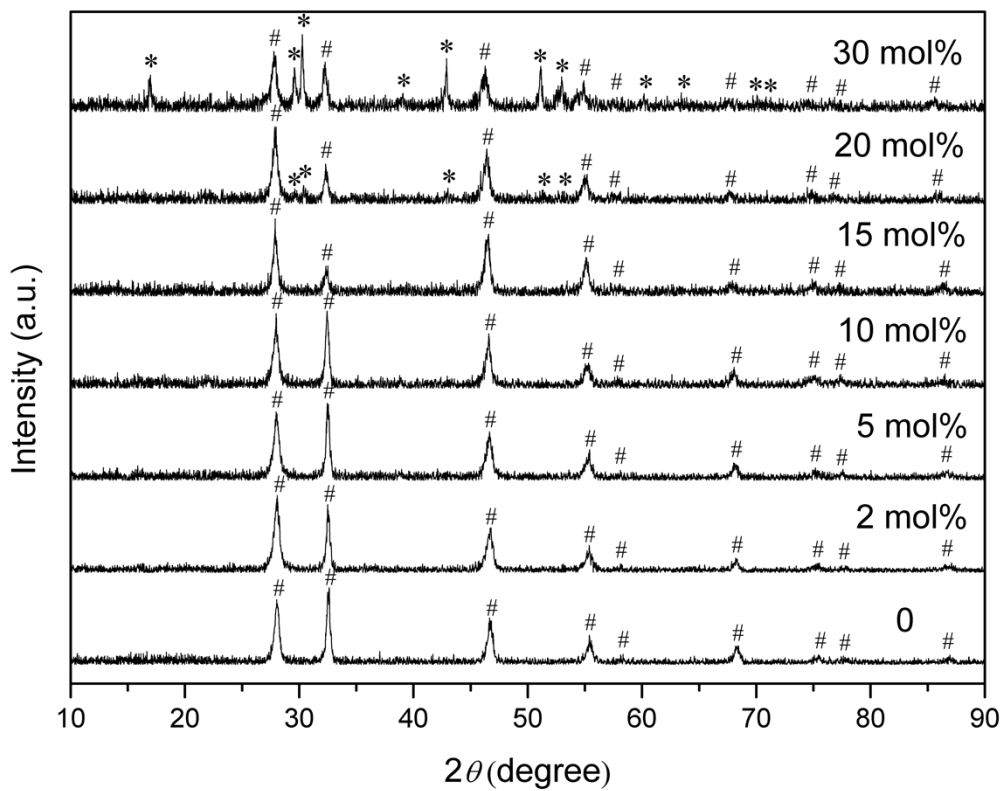


Fig. S4 XRD patterns of NaYF₄:Yb³⁺/Mn²⁺/Eu³⁺ (5/30/z mol%) (z = 0-30) NCs.

Symbols # and * represent the standard diffraction peaks of α-NaYF₄ and β-NaYF₄.

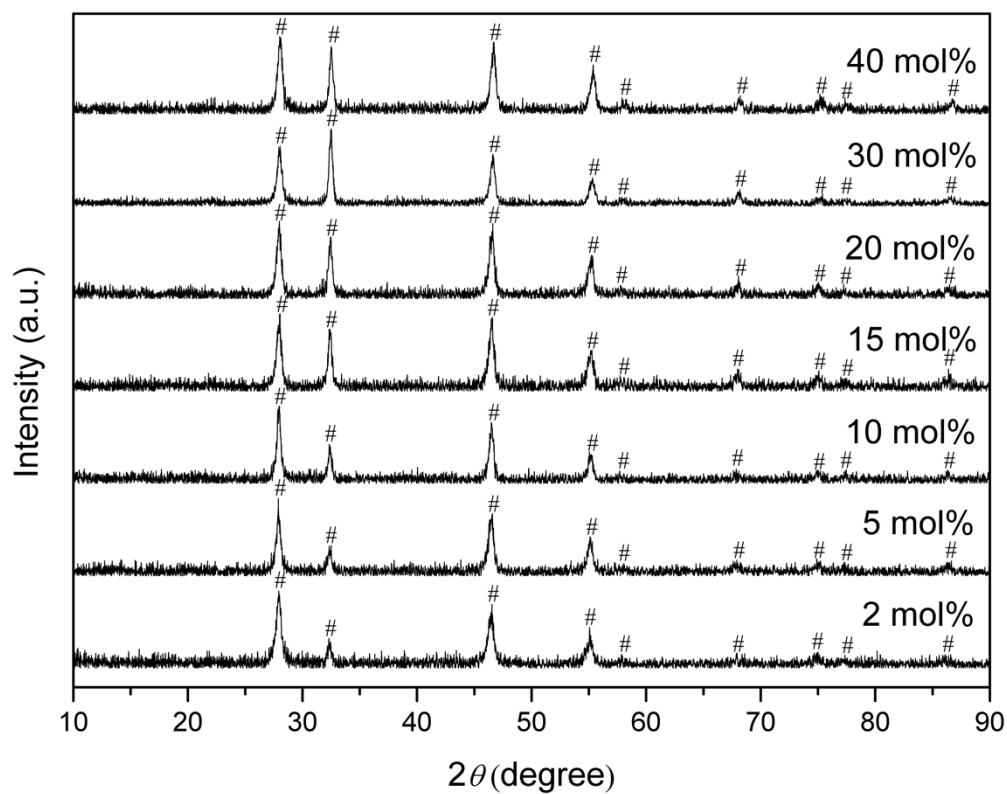


Fig. S5 XRD patterns of NaYF₄:Yb³⁺/Mn²⁺/Eu³⁺ (x/30/15 mol%) (x = 2-40) NCs.

Symbol # represents the standard diffraction peaks of α-NaYF₄.

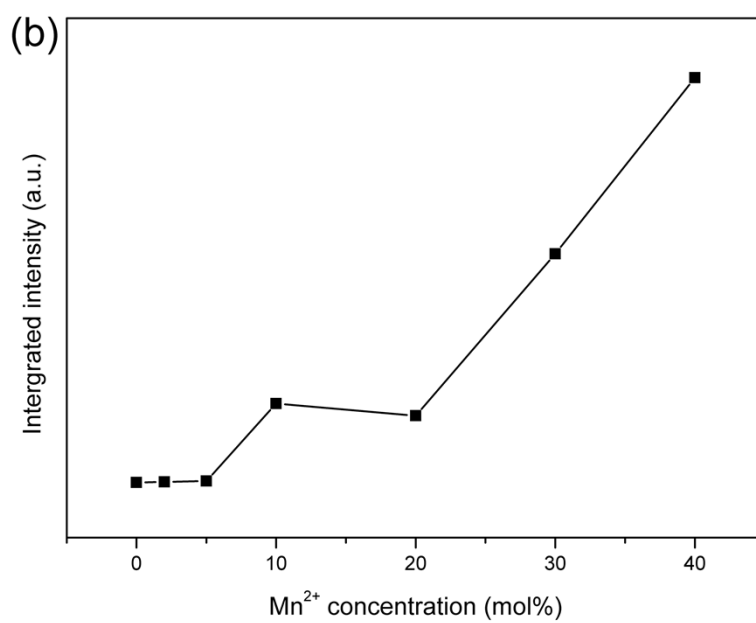
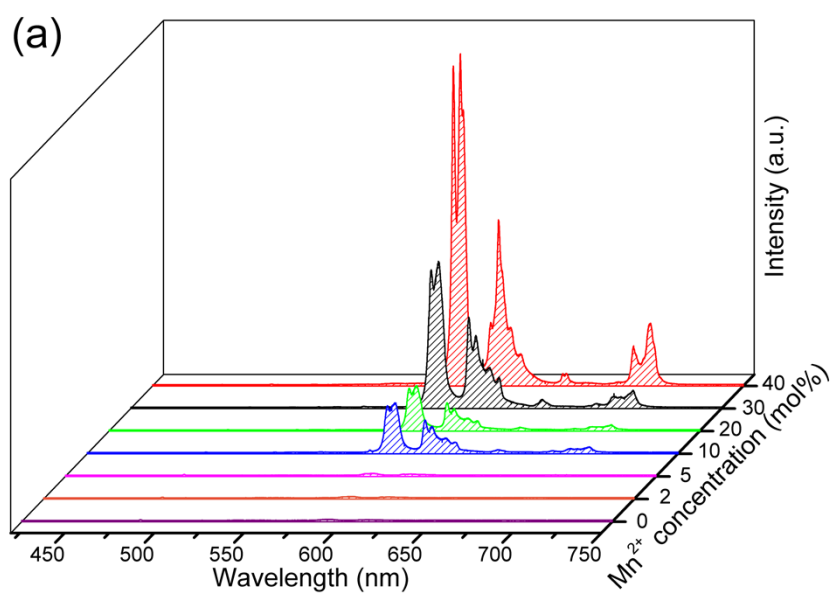


Fig. S6 (a) UCL emission spectra of NaYF₄:Yb³⁺/Mn²⁺/Eu³⁺ (5/y/15 mol%) (y = 0-40) NCs and (b) corresponding integrated intensity.

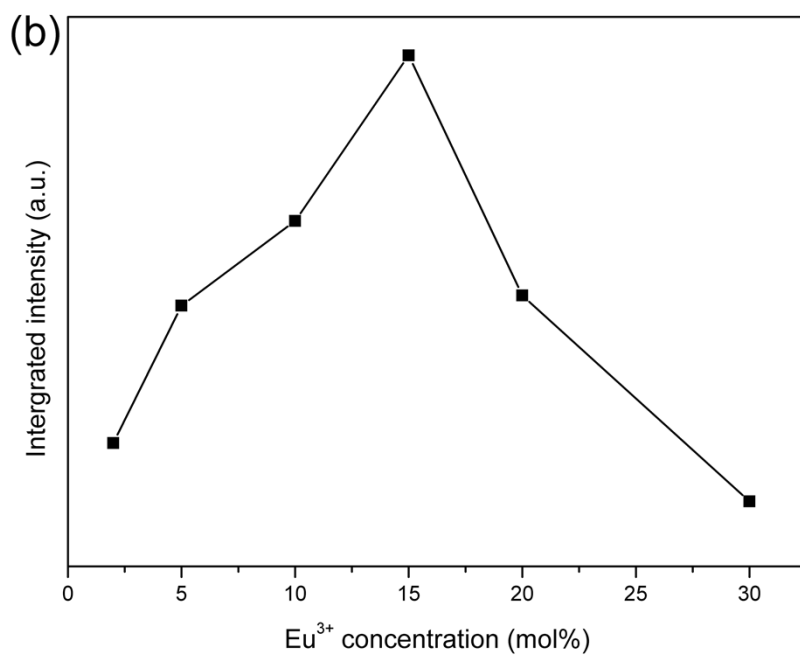
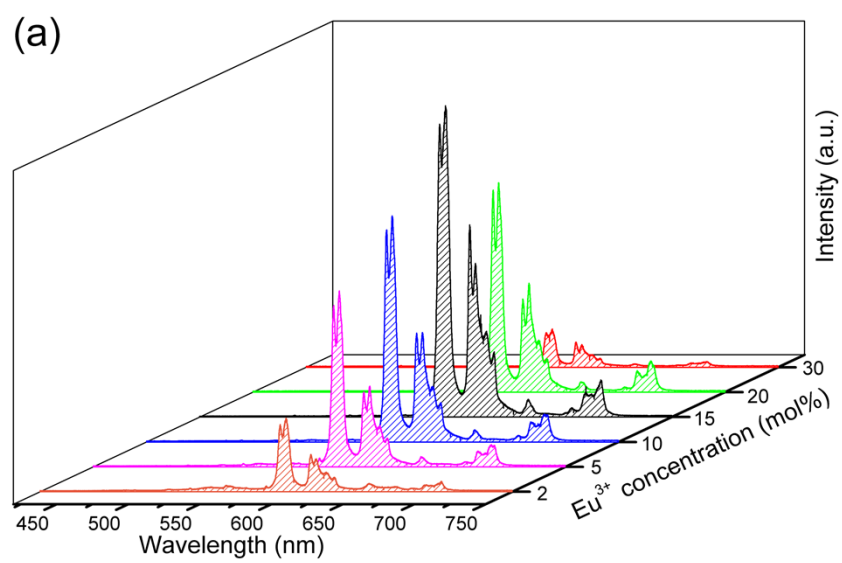


Fig. S7 (a) UCL emission spectra of NaYF₄:Yb³⁺/Mn²⁺/Eu³⁺ (5/30/z mol%) (z = 2-30) NCs and (b) corresponding integrated intensity.

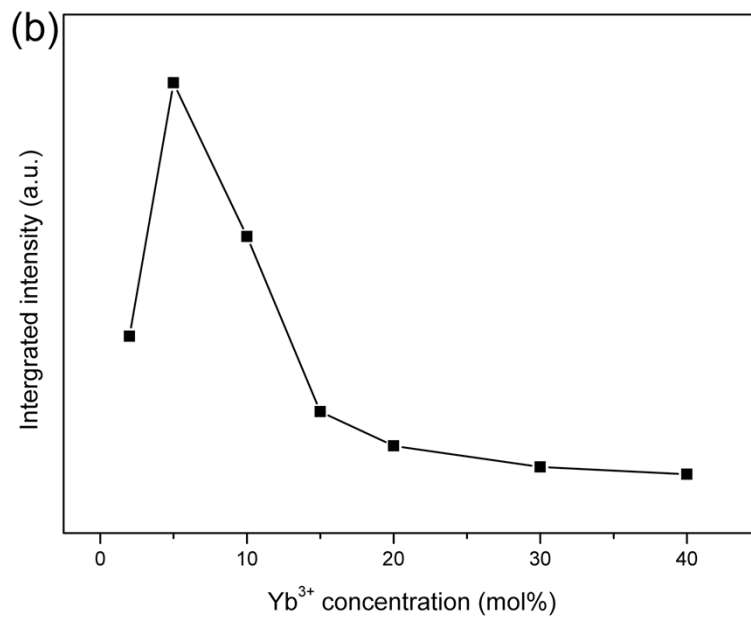
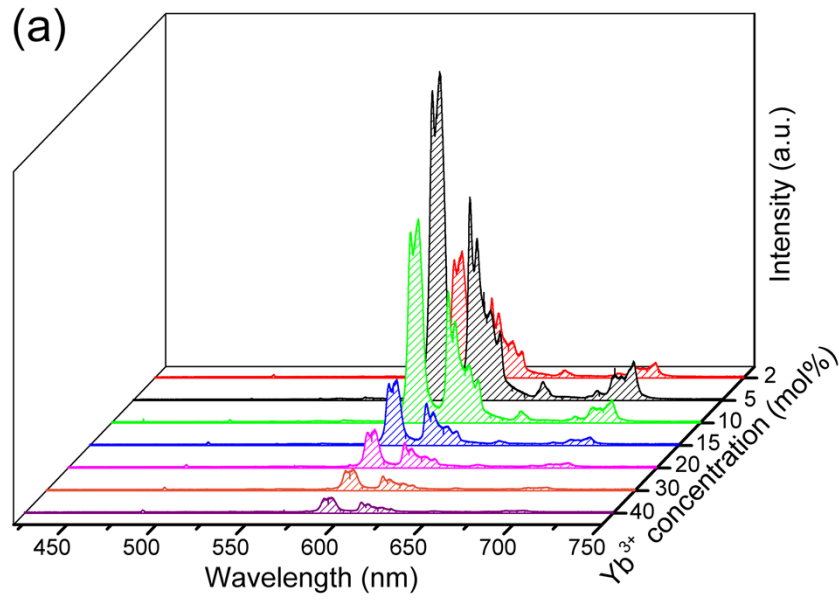


Fig. S8 (a) UCL emission spectra of NaYF₄:Yb³⁺/Mn²⁺/Eu³⁺ (x/30/15 mol%) (x = 2-40) NCs and (b) corresponding integrated intensity.

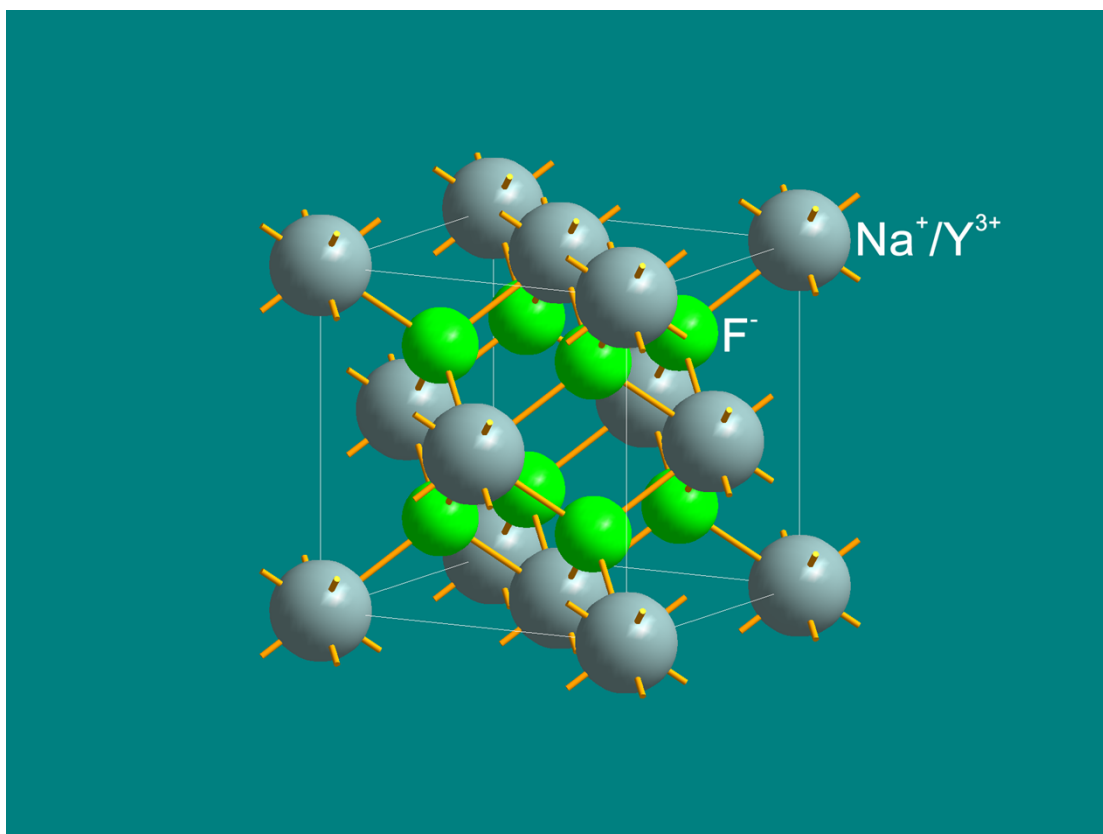


Fig. S9 Crystallographic structure of α - NaYF_4 according to ICSD 60257, Na^+ and Y^{3+} cations are randomly distributed in the cationic sublattice.

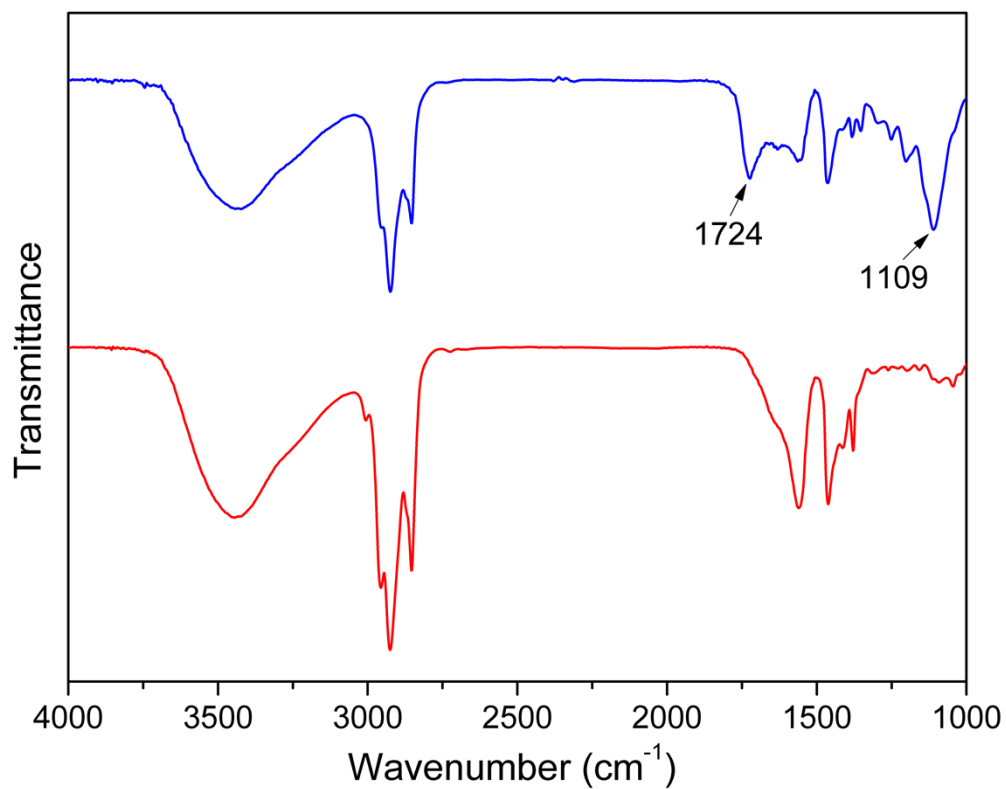


Fig. S10 FT-IR spectra of OA-UCNCs (red curve) and PEG-UCNCs (blue curve).

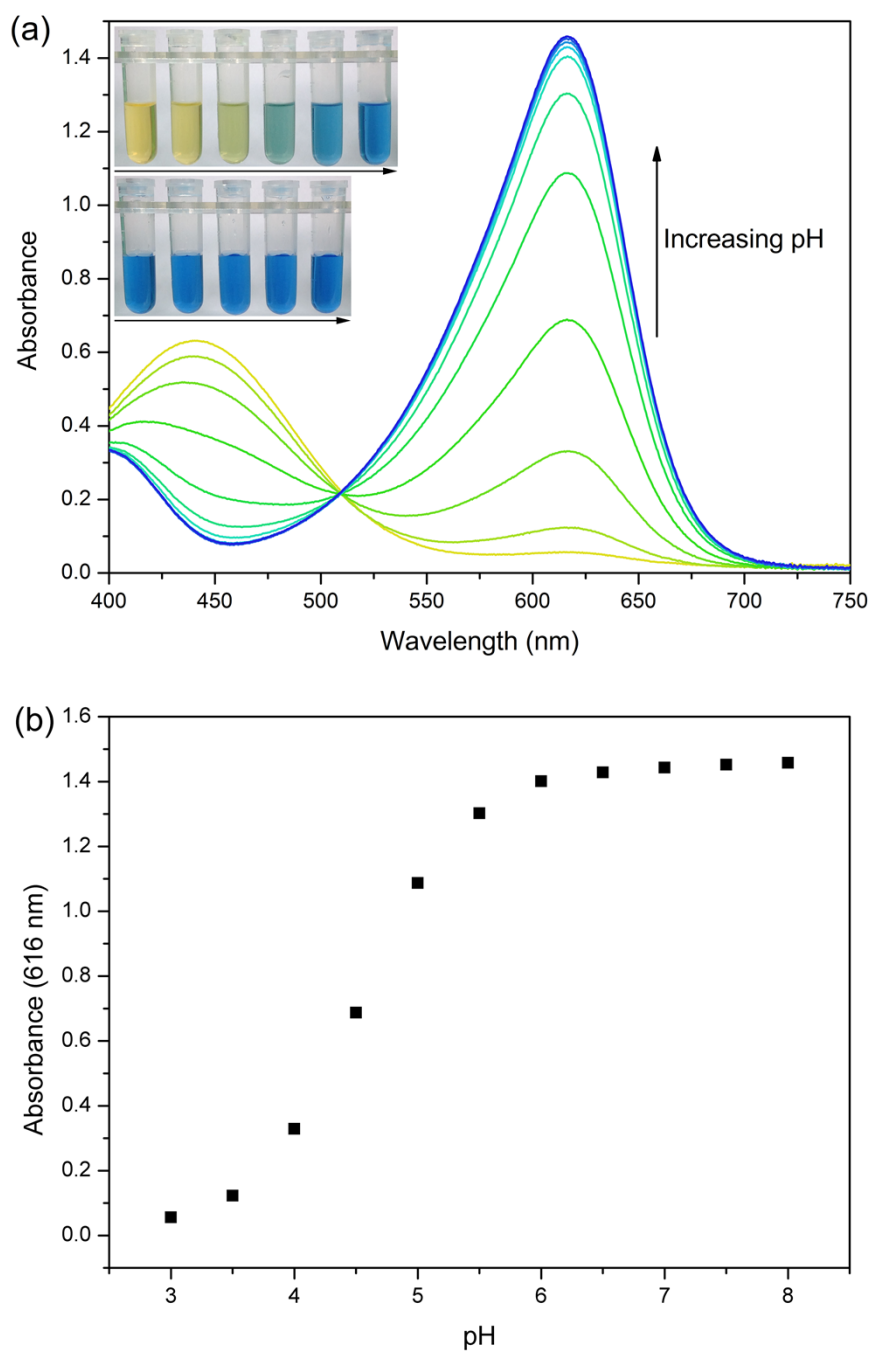


Fig. S11 (a) Absorption spectra and corresponding photographs of BCG in buffer solutions of different pH values and (b) absorbance at 616 nm with increasing pH values.

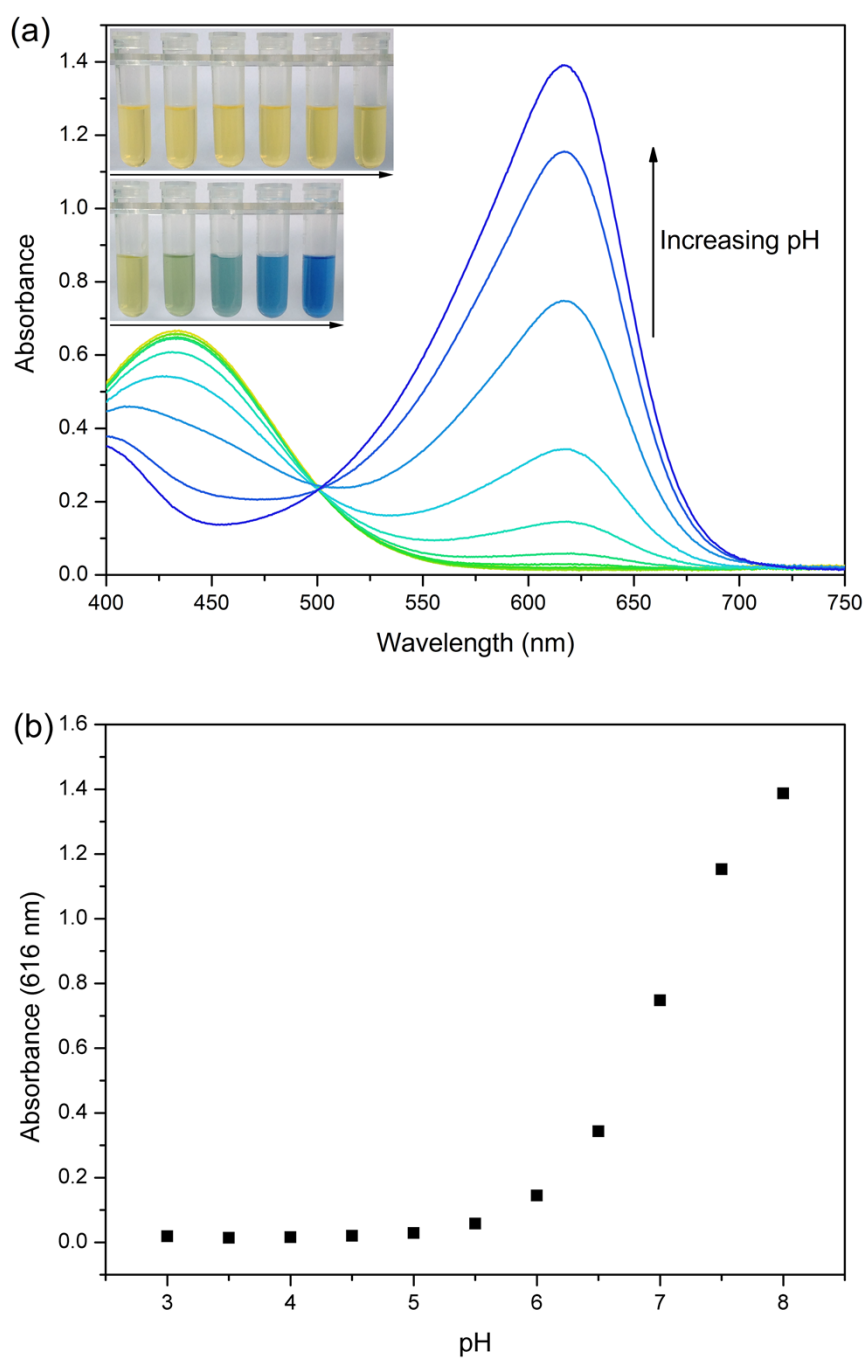


Fig. S12 (a) Absorption spectra and corresponding photographs of BTB in buffer solutions of different pH values and (b) absorption at 616 nm with increasing pH values.

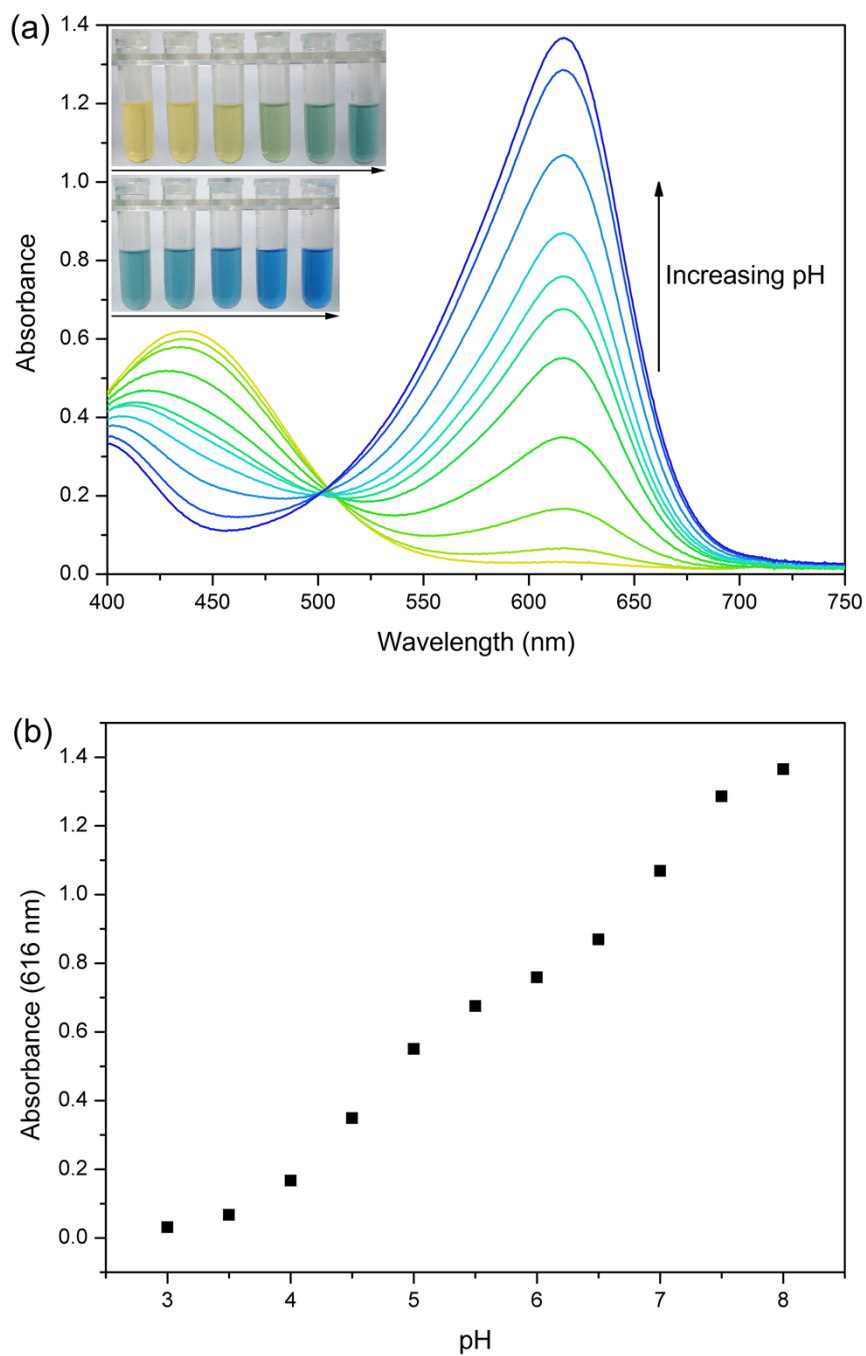


Fig. S13 (a) Absorption spectra and corresponding photographs of BCG and BTB mixture (mass ratio = 1:1) in buffer solutions of different pH values and (b) absorbance at 616 nm with increasing pH values.

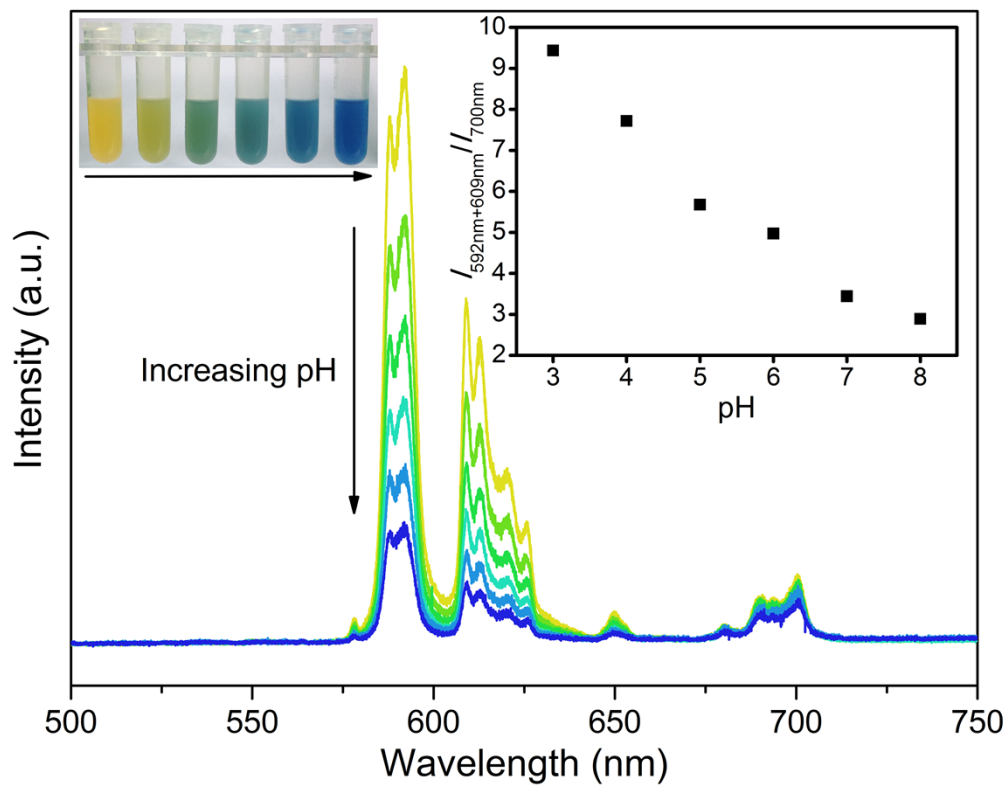


Fig. S14 UCL spectra and corresponding photographs of PEG-UCNCs with BCG and BTB mixture in buffer solutions of different pH values and the ratio of integrated intensity of ${}^5D_0 \rightarrow {}^7F_1$ (592 nm) plus ${}^5D_0 \rightarrow {}^7F_2$ (609 nm) to ${}^5D_0 \rightarrow {}^7F_4$ (700 nm) at different pH values (inset).

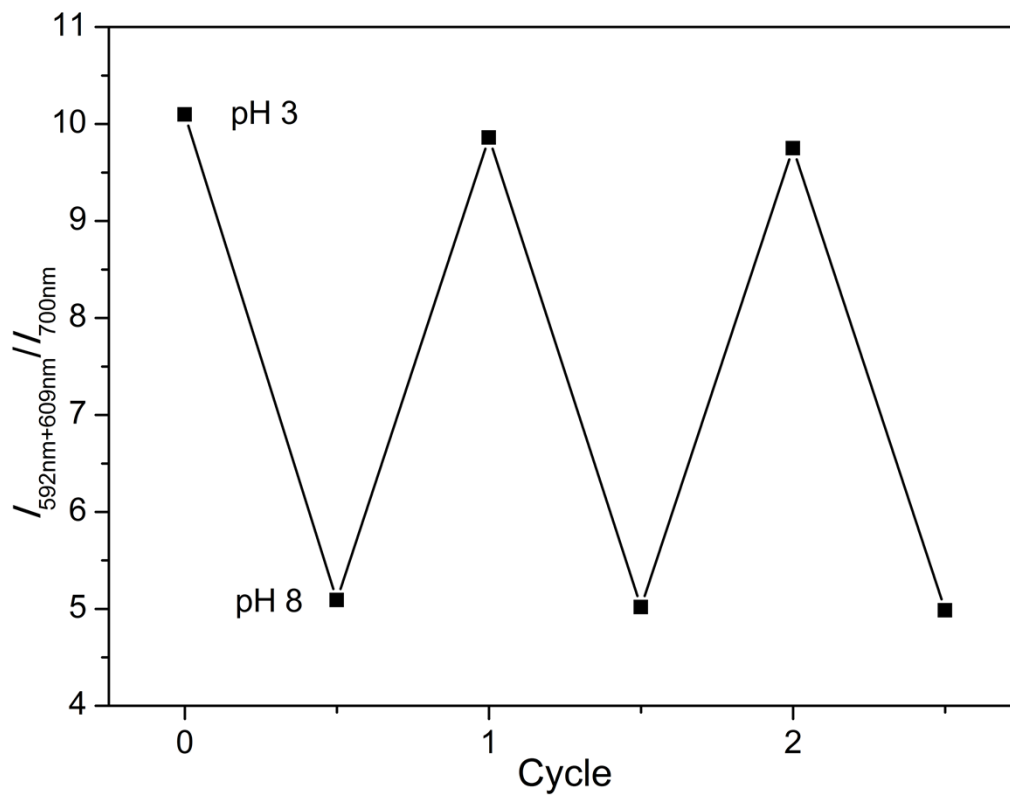


Fig. S15 The ratio of integrated intensity of ${}^5\text{D}_0 \rightarrow {}^7\text{F}_1$ (592 nm) plus ${}^5\text{D}_0 \rightarrow {}^7\text{F}_2$ (609 nm) to ${}^5\text{D}_0 \rightarrow {}^7\text{F}_4$ (700 nm) of the sensor film in buffer solutions of pH 3 and pH 8 for several cycles.